Science and Technology Indonesia
e-ISSN:2580-4391 *p*-ISSN:2580-4405
Vol. 10, No. 1, January 2025

Research Paper

Enhanced Performance of Epoxy Resin-Polyimide Hybrid Composites with Aminated Carbon Nanofibers Filler

Teguh Endah Saraswati[1*], Dini Deviana Saputri[1], Wijang Wisnu Raharjo[2]

[1]*Department of Chemistry, Faculty of Mathematics and Natural Sciences, Sebelas Maret University, Surakarta, 57126, Indonesia*
[2]*Department of Mechanical Engineering, Faculty of Engineering, Sebelas Maret University, Surakarta, 57126, Indonesia*
***Corresponding author**: teguh@mipa.uns.ac.id

Abstract
Incorporating epoxy resin (ER) and polyimide (PI) with supporting filler will exhibit composites with exceptional mechanical, thermal, and electromagnetic shielding properties. This research investigates the preparation of aminated carbon nanofiber (CNF) as a filler in epoxy resin-polyimide hybrid composites. The preparation of the CNF filler was initially done by the purification process through dissolution in toluene and vacuum annealing at 800°C for 3 hours. The amine modification of CNF was done by reacting CNF with ethylenediamine, sodium nitrite, and sulfuric acid. The aminated CNF was then mixed with polyimide precursor (oxydianiline and pyromellitic dianhydride), becoming poly(amic acid)-filler. The last step was combining poly(amic acid)-filler with epoxy resin diglycidyl ether bisphenol A and polyaminoamide as hardener. The Scanning Electron Microscope (SEM) and Transmission Electron Microscopy (TEM) images of CNF showed the overlapped bundle fibers with the average fiber diameter around 100-120 nm. The successful amine modification was analyzed through Fourier-Transform Infrared (FTIR) analysis by the functional group emergence of C–N (~1153 cm^{-1}), N–H (3737 cm^{-1}), primary amine N–H (1534 cm^{-1}), and better dispersion in water. The aminated filler shows a better distribution in the polymer matrices observed through macroscopic images and a higher hardness value. The FTIR of composites shows the increasing intensity in the N–H, C=O amide, and C–H functional groups, indicating the highly covalent bonds between polymers and the aminated CNF filler. The TGA graph shows the recognizable termination of the polyimide and epoxy resin matrices as major components in the composite. The ER-PI composites with aminated CNF filler show improved mechanical properties in the hardness, tensile properties, and electromagnetic interference (EMI) shielding efficiency by around three-fold higher than composites with unmodified CNF filler.

Keywords
Carbon Nanofiber, Amine Modification, Epoxy Resin, Polyimide, Composites

Received: 28 June 2024, Accepted: 10 October 2024
https://doi.org/10.26554/sti.2025.10.1.152-164

1. INTRODUCTION

Composites have become one of the trending materials used as building components in manufacturing industries. Composite materials show their rising demand as they bring increasing roles in various industry segments like automotive (Ravishankar et al., 2019), aerospace (Yadav et al., 2020), defense and space (Potluri and Krishna, 2020), marine (Mieloszyk et al., 2021), and consumer products (Todor et al., 2018), leading for composite material's rapid growth in engineering and material sciences. Their attractive combination has incredible characteristics, such as lightweight, toughness, high specific strength, stiffness, corrosion resistance, high strength, design flexibility, and durability (Lincon and Chalivendra, 2023; Rajak et al., 2019; Tri-Dung, 2020). Composite material consists of two or more constituent materials assembling a matrix with improved physical and chemical properties that can be further reinforced with other constituents called fillers (Hsissou et al., 2021; Krauklis et al., 2021). Composites have replaced the metal era because they are corrosion-resistant and lightweight, decreasing manufacturing costs (Egbo, 2021). Compared to metal-matrix and ceramic-matrix composites, polymer matrix composites have many advantages in their fabrication process due to their relatively low processing temperatures (Oladele et al., 2020). For example, carbon fiber-reinforced polymer (CFRP) and glass fiber-reinforced polymer (GFRP) become the most commercial systems in industry application because of their incredible properties (de Souza and Tarpani, 2021). Composites with electrical conducting properties have emerged as attractive electromagnetic interference (EMI) shielding materials (Kausar, 2020). The EMI shielding materials are generally

used to protect, prevent, and reduce the radiation of electromagnetic waves (Kondawar and Modak, 2020). The novel conductive fiber-reinforced polymer composites that achieve lightweight, high excellent strength, corrosion resistance, easy processing, and excellent EMI shielding performances were developed to replace metal-based (nickel, copper, and stainless steel) (Liu et al., 2021; Wu et al., 2021; Zhang and Gu, 2022).

The polymers are classified into thermoset and thermoplastic polymers (Dhanasekar et al., 2022). Thermoplastic polymer leads to weight loss and is more damage-resistant than thermosetting composite (Unnikrishnan and Kavan, 2022)-the bond between molecules in thermosetting polymers formed due to the help of weak Van der Waals forces. Meanwhile, the molecules are connected by chemical bonds in thermoplastic polymers (Iuvshin et al., 2020). The polymer matrices mainly used in CFRP applications are epoxy-based, bismaleimide-based, and polyimide-based resins (Huang et al., 2023).

Polyimide (PI) is successful in gaining more attention as polymer matrix material in preparing composites for tribological, mechanical, and thermal applications, owing to its good wear resistance, corrosion resistance, high strength-to-weight ratio, good interfacial bonding, better thermal stability, and had great applications (Ogbonna et al., 2021). PI is used in different forms, such as film, fiber, nanofiber, membrane, foam, and adhesives in the aerospace industry, medical, electronic devices, and sensors (Sezer Hicyilmaz and Bedeloglu, 2021). PI shows a high heat resistance behavior facilitated by its aromatic ring structure, commonly used in high-temperature fuel cell applications. Therefore, PI is a good candidate for manufacturing engineering parts due to its reasonable ability of excellent dielectric constant, tensile strength, elastic modulus, and adhesive properties (Ogbonna et al., 2021). PI consists of aromatic heterocyclics with an imide chain in its repeating unit of –CO–N–CO– and are synthesized through a reaction between dianhydride and diamine monomers (Zhou et al., 2023). The carbonyl group in the conjugated imide ring is symmetrical, limiting the mobility of free electrons in polyimide; thus, polyimide is suitable for insulation (Li et al., 2022).

Epoxy resin (ER) is a popular polymer for engineering composites that also exhibits excellent mechanical properties, chemical resistance, adhesive strength, insulating properties, resistance to thermal degradation, and chemical stability. ER also contains many hydrogen atoms, which are highly effective for attenuating neutrons (Elsafi et al., 2022; Qiao et al., 2022). One example of a well-known ER is diglycidyl ether of bisphenol A (DGEBA), formed by the condensation reaction of bisphenol A with epichlorohydrin (Hsissou et al., 2021). ER is widely applied as anticorrosion coatings because of their toughness, mechanical properties, and chemical-corrosion resistance. ER has high safety, low shrinkage on cure, and good adhesion to many substrates. However, ER's highly crosslinked chemical structure made them probably rigid and brittle, limiting their use in many applications (Jin et al., 2015). To overcome this limitation, ER can be combined with the other polymer, creating a hybrid polymer composite. ER has higher adhesive ability, and PI has higher flexibility, which could give synergetic properties to each other. Previous studies reported that incorporating ER and PI could potentially overcome each weakness, improving the composite properties (Chen et al., 2023; Li et al., 2024; Xu et al., 2023).

Matrix and filler are blended and combined in the composite to improve mechanical and physical properties (Kiran et al., 2018). Matrix and fillers can be adjusted to obtain desired properties. The tailoring of matrix and fillers may depend on their chemical structure, content, and synergetic interaction (Ahmed et al., 2020). Fillers could be formed as powders like metal oxide or ceramic and fibers like glass, carbon, or aramid (Thangavel et al., 2023). Several fillers in the incorporation with polyimide for engineering applications are inorganic oxides (SiO_2, Al_2O_3, TiO_2, ZnO_2, ZrO_2), carbon nanotubes, graphene, graphene oxide, boron nitride (BN), molybdenum disulfide (MoS_2), ionic liquids, carbon fibers, aramid fiber, glass fiber, silicon nitride (Si_2N_4), and carbon nitride (C_3N_4) (Ogbonna et al., 2023). Adding thermally conductive fillers to the polymer matrices in the microelectronic field prepares hybrid polymer composites with thermal resistance and conductive properties (Pan et al., 2021). Moaseri et al. (2014) developed hybridized carbon nanotubes/epoxy composites to improve fatigue life due to the strong bonding between epoxy and nanotubes in the interphase region of the composite (Bilisik et al., 2022).

Carbon allotropes with dominant sp^2 hybridized C atoms are well-known as good conductive fillers. This sp^2-structured carbon with a graphene network of carbon atoms is potentially used as a filler because it significantly improves polymers' thermal, physical, and mechanical properties even with low filler loading (Tarhini and Tehrani-Bagha, 2023). Carbon nanofiber (CNF) is one of the favorable carbon nanomaterials categorized as 1D nanomaterial with a structure more complicated than the single carbon nanotube (CNT). CNF is potentially applied in materials science, nanotechnology, energy storage, biomedicine, engineering, and environmental science due to its unique structure, function, and properties. As a sp^2-based discontinuous linear network, each layer's direction of CNF determines its mechanical properties. CNF can be categorized as CNF with various forms, such as hollow, porous, twisted, stacked, and helical structures (Wang et al., 2019; Yadav et al., 2020; Zhou et al., 2020).

Unfortunately, the main limitation of CNF is the tendency of their agglomeration into bundles because of siginificant Van der Waals forces between the filters: thus, it makes poor dispersion within the matrix due to low binding afinity (Lavagna et al., 2021). The way to overcome this limitation is by functionalizing CNF to increase carbon dispersion in the polymer matrix and improve interface interaction with the polymer (Lim et al., 2021) via covalent and non-covalent surface functionalization routes (Chen et al., 2019). Chemical modification is one of the effective ways of carbon functionalization through inserting functional groups (carboxylic, carbonyl, hydroxyl, and amine group) into the side walls of the carbon structure's surface as

well as to improve their interaction and reactivity with polymers by hydrogen bonding interaction (Mohd Nurazzi et al., 2021).

Fabrication of epoxy resin and polyimide as hybrid matrices polymer shows interesting potential ideas for creating fascinating hybrid composites with good mechanical, thermal, and electromagnetic shielding ability. However, the reported study still investigated polyimide addition less than 10%. Meanwhile, the polyimide's addition possibly provides interesting physical characteristics. Moreover, the modification of epoxy resin-polyimide composite using carbon nanomaterial as filler has not been widely studied, primarily related to the electromagnetic shielding properties.

Therefore, this study investigates the modification of CNF as fillers to enhance the performance of epoxy resin-polyimide composites. The CNF was modified by adding amine groups to improve their dispersion when mixed in epoxy resin-polyimide hybrid composites. The CNF was synthesized through the chemical vapor deposition method using an Incoloy catalyst at 800°C and purified before modification. The amine modification was done by radical reaction with ethylenediamine, sodium nitrite, and sulfuric acid. The unmodified and aminated CNF were then used as filler in the epoxy resin-polyimide hybrid composites, and the resulting composites were further studied.

2. EXPERIMENTAL SECTION

2.1 Materials

The materials used in this research were toluene (Merck, 99.9%), ethanol (Merck, technical grade), ethanol (Merck, 99%), ethylene diamine (Merck, 99.9%), sodium nitrite (Honeywell, Riedel-de Haën, 99%, density of 2.17 g/cm^3), sodium dodecyl sulfate (Merck, 97%, molecular weight of 288.38 g/mol), sulfuric acid (Merck, 98%, molecular weight of 98.08 g/mol)), dimethylformamide (Merck, 99%, molecular weight of 73.09 g/mol), 4,4'-oxydianiline (Tianjin Icason Technology, 99.5%, molecular weight of 200.24 g/mol), pyromellitic dianhydride (Tianjin Icason Technology, 99.5%, molecular weight of 218.12 g/mol), dimethylacetamide (Merck, 99%, molecular weight of 87.12 g/mol), epoxy resin diglycidyl ether bisphenol A (DGEBA, Epichlorohydrin, Eposchon, Justus Kimiaraya Indonesia, density 1.17 ± 0.01 g/cm^3), and polyaminoamide (Hardener, Eposchon, Justus Kimiaraya Indonesia). Furnace OTF-1200X was used to perform the chemical vapor deposition (CVD) process for CNF preparation and the vacuum annealing process for CNF purification.

2.2 Preparation of Filler

The CNF was synthesized following our previous report (Setiawan et al., 2023). The CNF was then purified by soaking it in toluene 100 mL with ultrasonication for 20 minutes. The CNF was then separated from toluene by decantation. The CNF was re-soaked with ethanol, centrifuged, and dried using a vacuum chamber. Furthermore, the CNF underwent the vacuum annealing process at 800°C for 3 hours to get the purified CNF.

2.3 Amine Modification of CNF

The purified CNF (1 g) was aminated through the reaction with ethylenediamine (121.43 mg), sodium nitrite (132.86 mg), sulfuric acid (0.087 mL), and sodium dodecyl sulfate (121.43 mg). The mixture was mixed in heating condition at 60°C for 1 hour. The mixture was then washed with dimethylformamide (DMF) and distilled water to remove unreacted residual from the product.

2.4 Preparation of Composites

A precursor of polyimide (poly(amic) acid) was prepared through the reaction between 4,4'-oxydianiline (2.5 g) and filler (50 mg) in dimethylacetamide as solvent (35 mL) in ultrasonicator for 1 hour at room temperature. Then, the mixture was stirred in an ice bath for 15 min under a nitrogen atmosphere. Pyromellitic dianhydride (2.5 g) was added to the mixture and stirred for 60 min to gain the poly(amic acid) solution.

Poly(amic) acid-filler solution (2 mL) was then mixed with epoxy resin bisphenol A (6 g) in a continuous stirring process for 15 min. Polyaminoamide as a hardener was added to the final mixture and stirred until a homogenous mixture was obtained. All the mixture was molded and cured at 60°C for 12 hours or more until it entirely solidified.

2.5 Characterization

The purified and aminated CNF were characterized by Scanning electron microscope (SEM Hitachi SU3500), Transmission electron microscopy (TEM Tecnai G2 20S-Twin), X-ray diffraction (XRD Philips Analytical (Cu, 40.0 kV, 30.0 mA in the range 2θ of 10 – 90°), and Fourier transform infrared spectroscopy (FTIR), Shimadzu IR Prestige-21, measured in the wavenumber 400 – 4000 cm^{-1}). The resulting composites were characterized using a macroscopic testing tool (Olympus stereo microscope SZX7), Fourier transform infrared spectroscopy (FTIR) (Shimadzu IR Prestige-21, measured in the wavenumber 400-4000 cm^{-1}), durometer shore A and D, and Thermogravimetry analysis (TGA, Linseis STA PT 1600, analyzed at room temperature – 800°C), tensile strength test (JTM-UTS510 Universal testing machine based on ASTM D638). The electromagnetic radiation reduction test was carried out using an electromagnetic radiation detector DT-1130).

3. RESULT AND DISCUSSION

CNF was successfully synthesized through the CVD method using an Incoloy catalyst at 800°C. During the synthesis process, some impurities, such as amorphous carbon, graphitic nanoparticles, fullerenes, and metal particles from the catalysts – typically Fe, Co, and Cr are contained in Incoloy catalyst (Manikandan et al., 2017), could be formed and disrupt the physical and chemical properties of CNF. These impurities can be removed by the purification process. The purification process was conducted using toluene and ethanol – no acid was used to avoid removing the magnetic properties, and the process was followed by drying with vacuum annealing. After this process, the tubular graphitic CNF structures are more

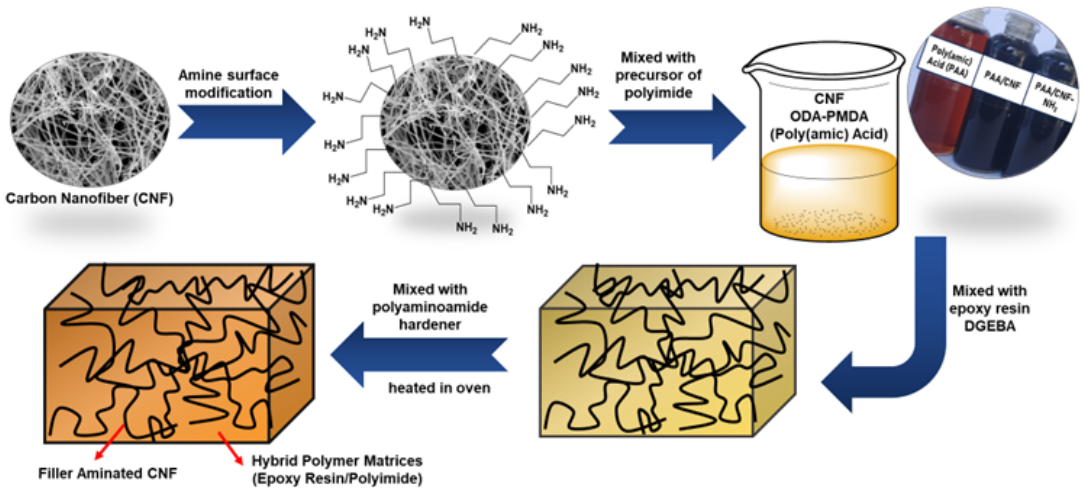

Figure 1. Schematic Representation of Preparation Epoxy Resin-Polyimide Composites with CNF Filler

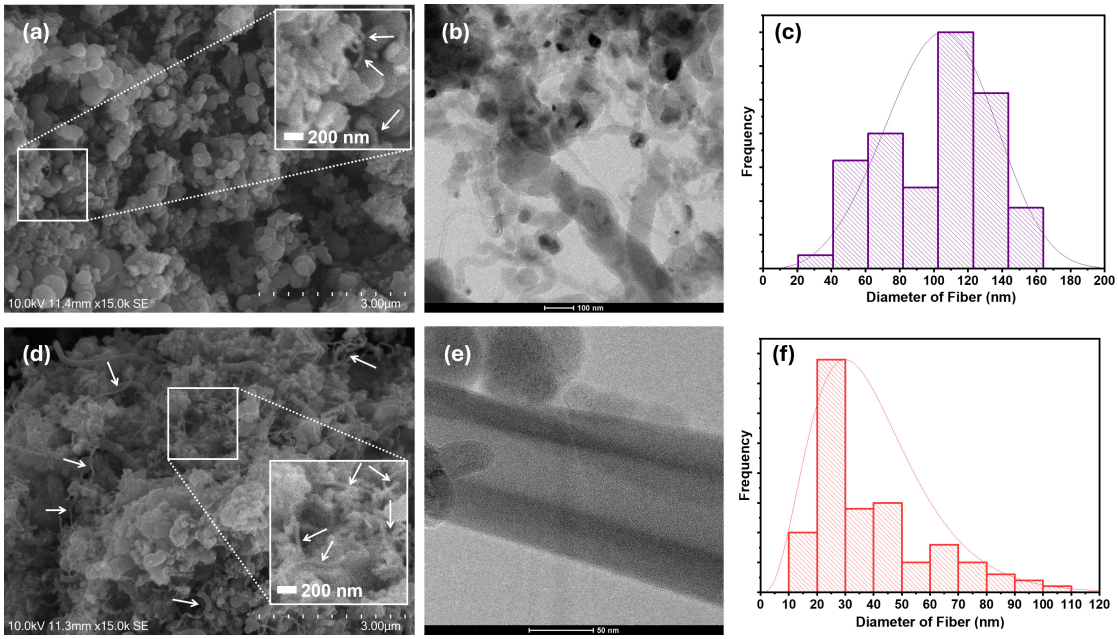

Figure 2. Synthesized of CNF filler: Before Purification (a) SEM Images, (b) TEM Images, (c) Histogram of Diameter's Fiber, and After Purification (d) SEM Images, (e) TEM Images, (f) Histogram of Diameter's Fiber

significantly observable than before purification (Ribeiro et al., 2021). Purified CNF was then modified to attach amine functional groups to the side wall of its structure, which hopefully can increase dispersion characteristics and prevent aggregation. Aminated CNF filler was then mixed with poly(amic) acid as a precursor agent of polyimide and was further mixed with epoxy resin and hardener, forming the final composites. The schematic representation of composite preparation is shown in Figure 1.

Scanning electron microscope (SEM) and Transmission electron microscopy (TEM) images of synthesized CNF accompanied by their histogram before and after purification are presented in Figure 2 (a-f). The CNF shows the aggregation that the CNF looks like bundle fibers overlapping. These agglomerates result from entanglement and aggregation between individual nanofibers (Khattak et al., 2013). After purification, the agglomerates decrease; therefore, more nanofiber appears with the individual long tube characteristic. The TEM images show the CNF tube's mean diameter before purification of 100-120 nm is wider than its diameter after purification of 20-30 nm.

The X-ray diffraction patterns of purified and aminated CNF are shown in Figure 3. The purified and aminated CNF shows three main components: carbon, iron oxide, and iron car-

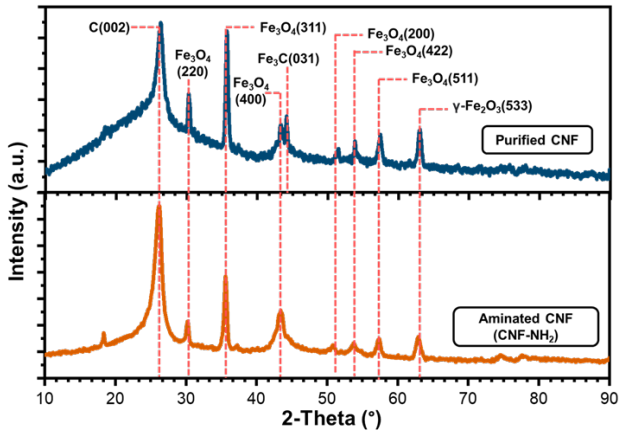

Figure 3. XRD Analysis of Purified CNF and Aminated CNF

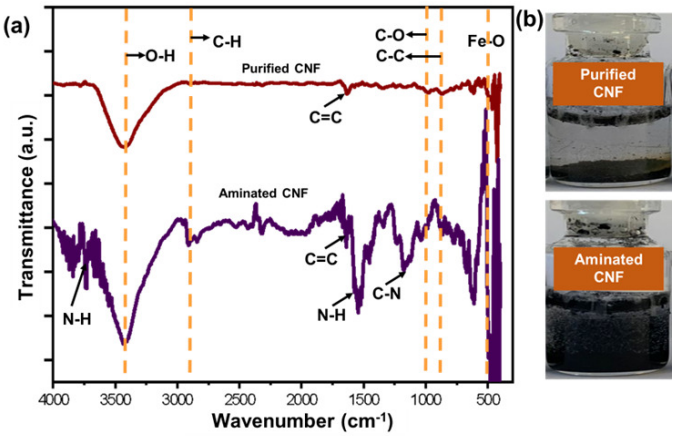

Figure 4. (a) FTIR Spectra and (b) Dispersity of Purified CNF and Aminated CNF in Water

bide. Carbon peak C(002) based on PDF #75-1621 (graphite) is observable as a peak in high intensity at an angle of 2θ 26.25°. The Fe_3C peak observed in purified CNF at an angle of 2θ 44.09° (031) (referred to PDF #77-0255 (Fe_3C)) was not observed in aminated CNF. Iron oxide, possibly coming from an Incoloy catalyst, is observable in both purified and aminated CNF, which reveals three phases: Fe_3O_4 (magnetite), α-Fe_2O_3 (hematite), and γ-Fe_2O_3 (maghemite). Both purified and aminated CNF show the Fe_3O_4 peak at an angle of 2θ 30.26° (220), 35.74° (311), 43.38° (400), 51.41° (200), 53.93° (422), 57.33° (511), analyzed based on PDF #89-0691 (Fe_3O_4). Both purified and aminated CNF also show γ-Fe_2O_3 peak at 2θ 63.15° (553), referred to PDF #39-1346 (γ-Fe_2O_3). The maintained iron oxide phases indicate that the amine surface modification did not destroy the crystalline structure of aminated CNF, as the tube structures of CNF are still preserved.

The Fourier transform infrared (FTIR) spectra were characterized to confirm the successful amine surface modification, shown in Figure 4 (a). The purified CNF reveals some peaks, such as Fe–O (~450-600 cm^{-1}), C–O (~1117 cm^{-1}), C=C (~1630 cm^{-1}), C–H (~2900 cm^{-1}), O–H (~3000-3500 cm^{-1}) (Havigh and Chenari, 2023; Kanjana et al., 2023). The aminated CNF reveals some peaks of C–N (~1100-1350 cm^{-1}), N–H (3200-3800 cm^{-1}) (Mokhtarifar et al., 2017), and primary amine N–H (1540 cm^{-1}) (Eren et al., 2015) that indicates the successful amine surface modification through covalent bonding of C–N and N–H functional group. Figure 4 (b) shows the dispersion test of CNF before and after amine surface modification. The result reveals that aminated CNF shows better dispersion in polar liquid (distilled water) than purified CNF. This improvement might be due to the attachment of hydrophilic amine groups, making the polar filler as they can homogenously disperse in water.

The aminated CNF (CNF−NH_2) was added as fillers into the epoxy resin and epoxy resin-polyimide composites. To study the influence of CNF surface modification on the mechanical properties, the unmodified CNF (CNF after purification) was also used separately as a filler for comparison. The macroscopic images test was used to characterize the surface morphology and the dispersion of CNF fillers in polymer composites of epoxy resin (ER) and epoxy resin-polyimide (ER-PI), as shown in Figure 5 (a) and (b), respectively. The macroscopic image of ER and ER-PI composites shown in Figure 5 (a and b) have a brighter color than the other composites reinforced with CNF and aminated CNF (CNF−NH_2) fillers such as ER/CNF, ER/CNF−NH_2, ER-PI/CNF, and ER-PI/CNF−NH_2. The black CNF fillers can significantly result in darker composites.

The macroscopic images of composites show fine voids possibly coming from gas bubbles formed due to air diffusion during polymer composites' stirring. Adding other polymer and filler components increases the matrix viscosity, causing the trapped air in the bubbles not to leave the polymer suspension (Hashemi and Mousavi, 2016). This phenomenon results in weak interfacial bonding within the polymers or between the polymers and filler, leading to severe destruction in composites (Kranauskaite et al., 2018). The non-homogeneous dispersion also possibly influenced this weak bonding interaction, as shown in the composites reinforced by unmodified CNF. On the other hand, less void was observed in the macroscopic image of ER/CNF−NH_2 and ER-PI/CNF−NH_2 composites due to the aminated CNF fillers being well dispersed in polymer matrices. The aminated CNF might reveal individual fibers interacting more with matrices than the non-aminated CNF filler. The more homogenous compound of composites will provide the higher interaction and performance of mechanical, electrical, and thermal properties.

The FTIR analysis of composite confirms the emergence of functional groups that build up composite structures. Figures 6 (a) and 6 (c) show the FTIR of ER and ER-PI composites, respectively, with unmodified and aminated CNF fillers. Figure 6 (a) and Figure 6 (c) show distinguished peaks after the addition of unmodified CNF and aminated CNF, including C=C (~1630 cm^{-1}), C–H (~2900 cm^{-1}) (Havigh and Chenari, 2023), and N–H at wavenumbers (3200-3800 cm^{-1}) (Mokhtar-

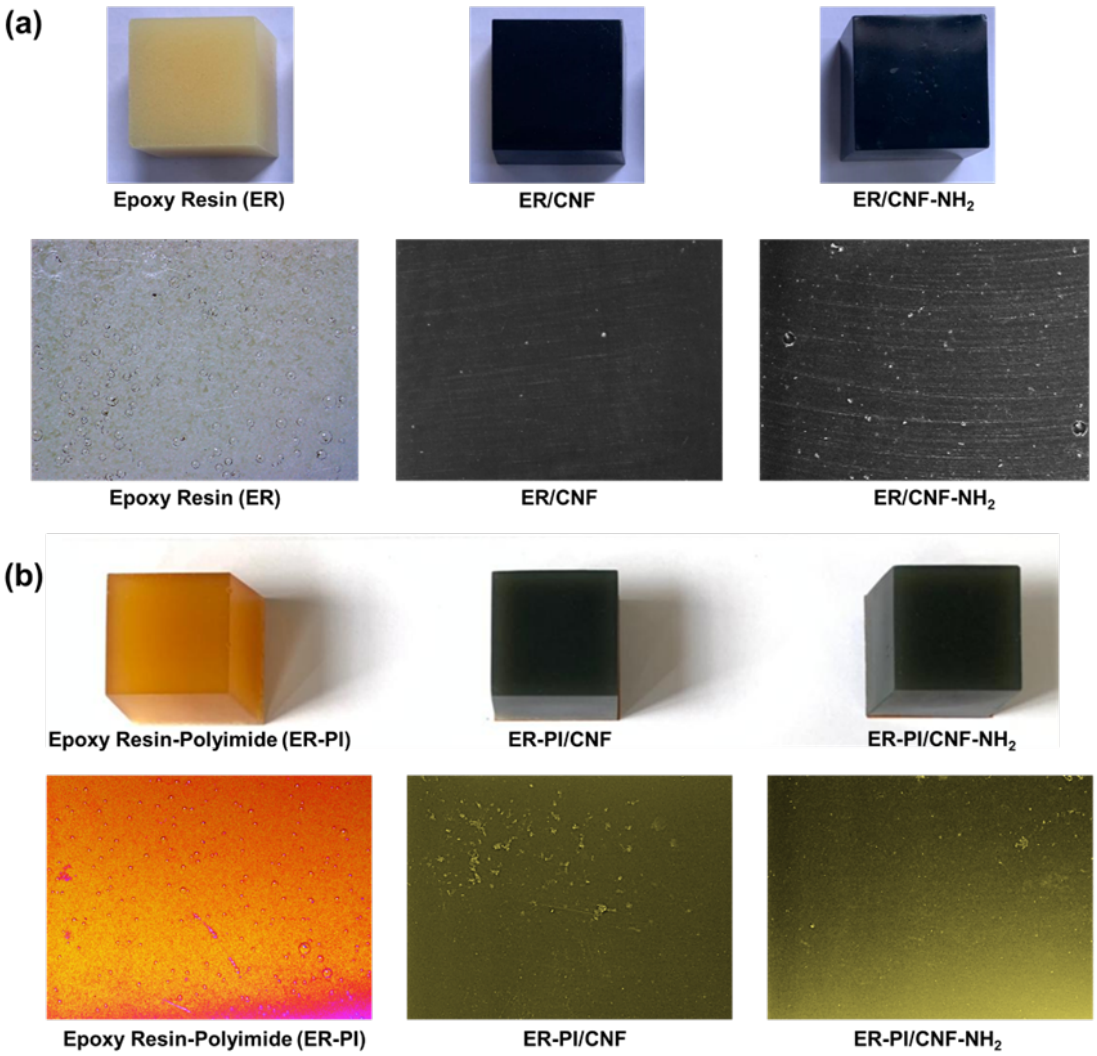

Figure 5. Macroscopic Images of the Composites (a) Epoxy Resin (ER) with CNF and Aminated CNF Filler, and (b) Epoxy Resin-Polyimide (ER-PI) with CNF and Aminated CNF Filler

ifar et al., 2017). The ER composites with unmodified and aminated CNF show the increasing intensity of the C=O epoxy group (~900-1050 cm^{-1}) (Duarah and Karak, 2015), while the ER-PI composites show the rising intensity of the C=O PI (~913-1000 cm^{-1}) (Chen et al., 2023). This increase is due to the merger of epoxy resin-polyimide with CNF filler connected by N−H and C=O groups. The increase in the intensity of the C−H group may come from C−H in carbon material (CNF).

The TGA graph of ER and ER-PI composites with filler are shown in Figures 6 (b) and 6 (d), respectively. Both figures show insignificant differences in degradation temperatures. This feature is probably due to the significant degradations of ER, PI, and polyaminoamide at ~342°C, ~479°C, and ~463°C, respectively. These thermal degradations were mainly due to the dissection of the C–N, C–O, and phenyl groups in ER and PI structures (Khan et al., 2021). The degradation representing CNF filler does not reveal significant degradation due to the small mass content in the composite. Table 1 shows the hardness value and the EMI absorption efficiency of the composites. A hardness test is a mechanical testing of material related to the resistance from penetrating forces (Abbass et al., 2020). Meanwhile, the EMI absorption efficiency test estimates the ability of the composites to absorb the electromagnetic waves coming out from the electronic instrument.

The hardness test shows that composite with aminated filler gives a higher value than others. The EMI absorption efficiency test was done by testing the electromagnetic radiation on the side wall of the refrigerator with and without the composites. In the EMI absorption efficiency test, a higher reduction of electromagnetic wave coming out the device was observed when the composite with aminated filler was used as shielding. The higher hardness value and EMI absorption are related to increasing the reinforcement ratio due to homogeneous distribution, concluding that aminated filler positively

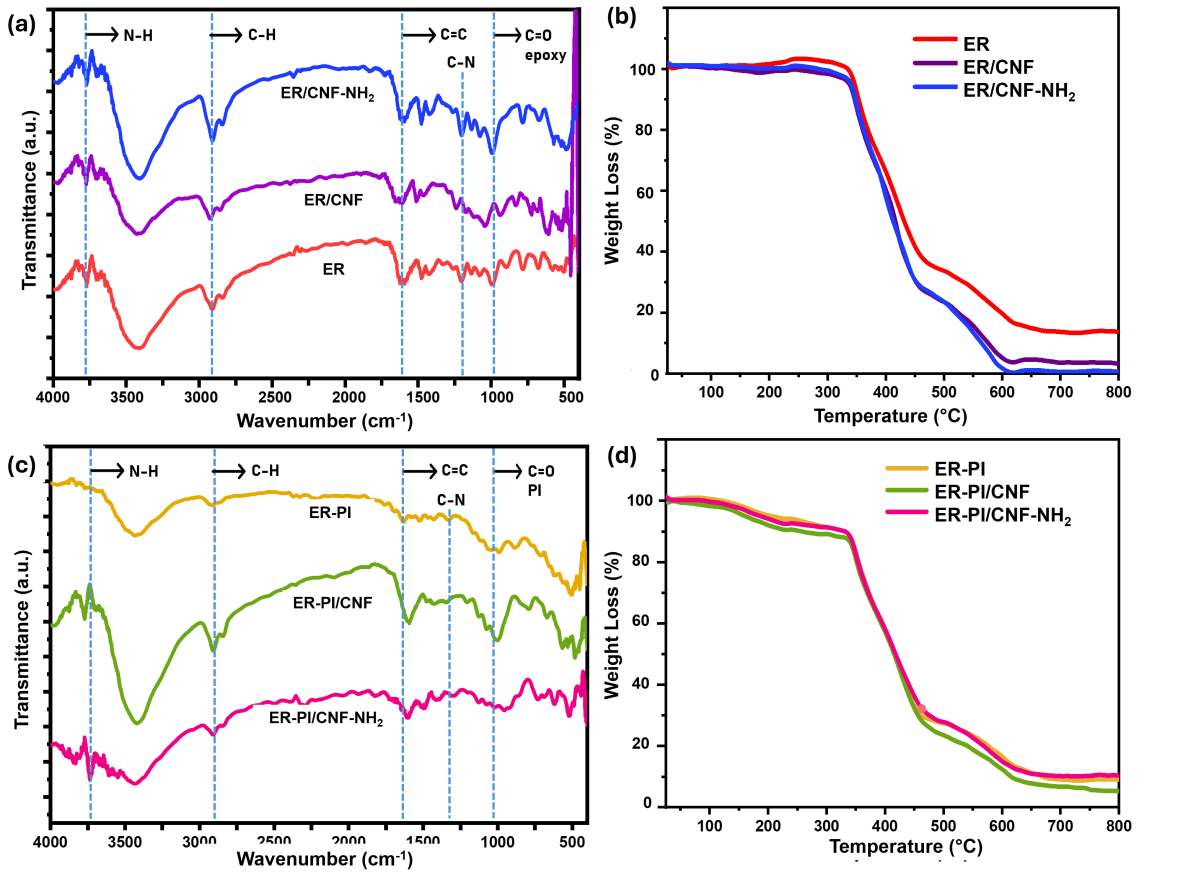

Figure 6. (a) FTIR Spectra of Epoxy Resin (ER) Composites, (b) TGA Analysis of Epoxy Resin (ER) Composites, (c) FTIR Spectra of Epoxy Resin-Polyimide (ER-PI) Composites, and (d) TGA Analysis of Epoxy Resin-Polyimide (ER-PI) Composites

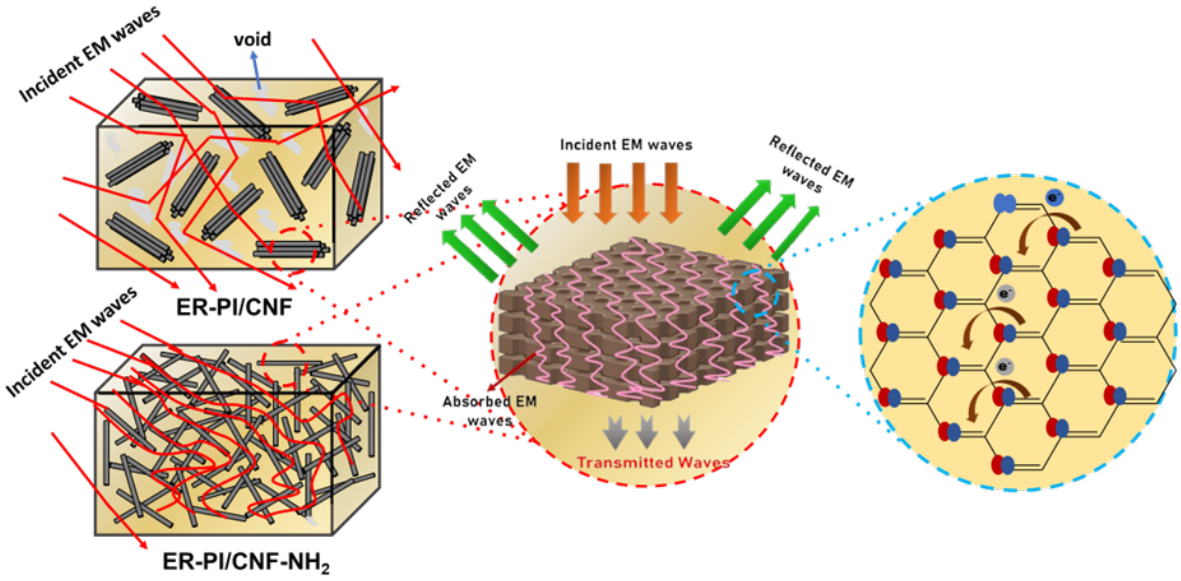

Figure 7. The Illustration of Composite ER-PI with Aminated CNF (CNF−NH_2) and Non-Aminated CNF during Absorbing the Electromagnetic Wave

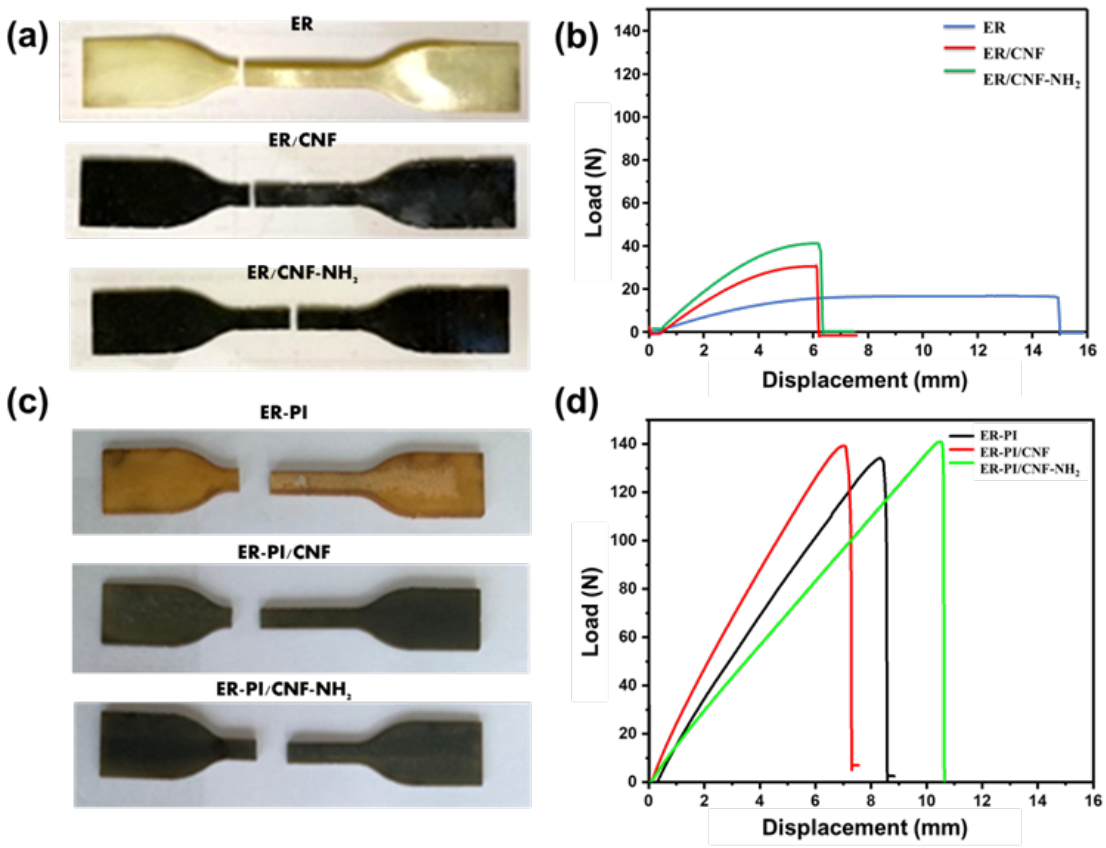

Figure 8. (a) Specimen for Tensile Test of Epoxy Resin Composites with CNF and Aminated CNF Filler, (b) Tensile Load and Displacement Curves of Epoxy Resin Composites with CNF and Aminated CNF Filler, (c) Specimen for Tensile Test of epoxy Resin-polyimide Composites with CNF and Aminated CNF Filler, and (d) Tensile Load and Displacement Curves of Epoxy Resin Composites with CNF and Aminated CNF Filler

Table 1. The Hardness and EMI Absorption Efficiency of Composites

Composites	Hardness Value	EMI Absorption Efficiency (%)
Epoxy Resin (ER)	62.17 ± 0.98 (HD)	24.210
ER/CNF	69 ± 0.63 (HD)	44.560
ER/CNF−NH_2	73.08 ± 0.58 (HD)	55.850
Epoxy Resin-Polyimide (ER-PI)	75.33 ± 0.60 (HA)	45.906
ER-PI/CNF	77.50 ± 0.55 (HA)	50.072
ER-PI/CNF−NH_2	79.42 ± 0.37 (HA)	70.644

impacts composite properties, including the EMI absorption efficiency, as illustrated in Figure 7. As illustrated in Figure 7, non-aminated CNF filler cannot be dispersed well in a polymer matrix (ER-PI/CNF), creating more voids, as observed in Figure 5. These voids make the electromagnetic wave easily escape; therefore, the electromagnetic wave cannot be trapped efficiently. The homogenously dispersed aminated CNF in the polymer matrix provides fewer voids for electromagnetic wave attenuation by multi-reflection and absorption, thus leading to higher absorption shielding. Therefore, ER-PI/CNF−NH_2 has a higher shielding ability than ER-PI/CNF.

Tensile strength was also tested to determine the mechanical properties of ER-PI composites with CNF and aminated CNF. Based on ASTM D638, the tensile specimens were formed as a dogbone-like shape in the type IV category and broken after testing, as shown in Figure 8 (a) and (c), respectively, for CNF fillers-reinforced ER and ER-PI composites. The tensile strength graphs of ER and ER-PI composites with CNF fillers are shown in Figure 8 (b) and (d). The maximum load value refers to the maximum stress the material can restrain while being stretched or pulled before breaking. As the tensile load increases, the material will deform elastically and will return to

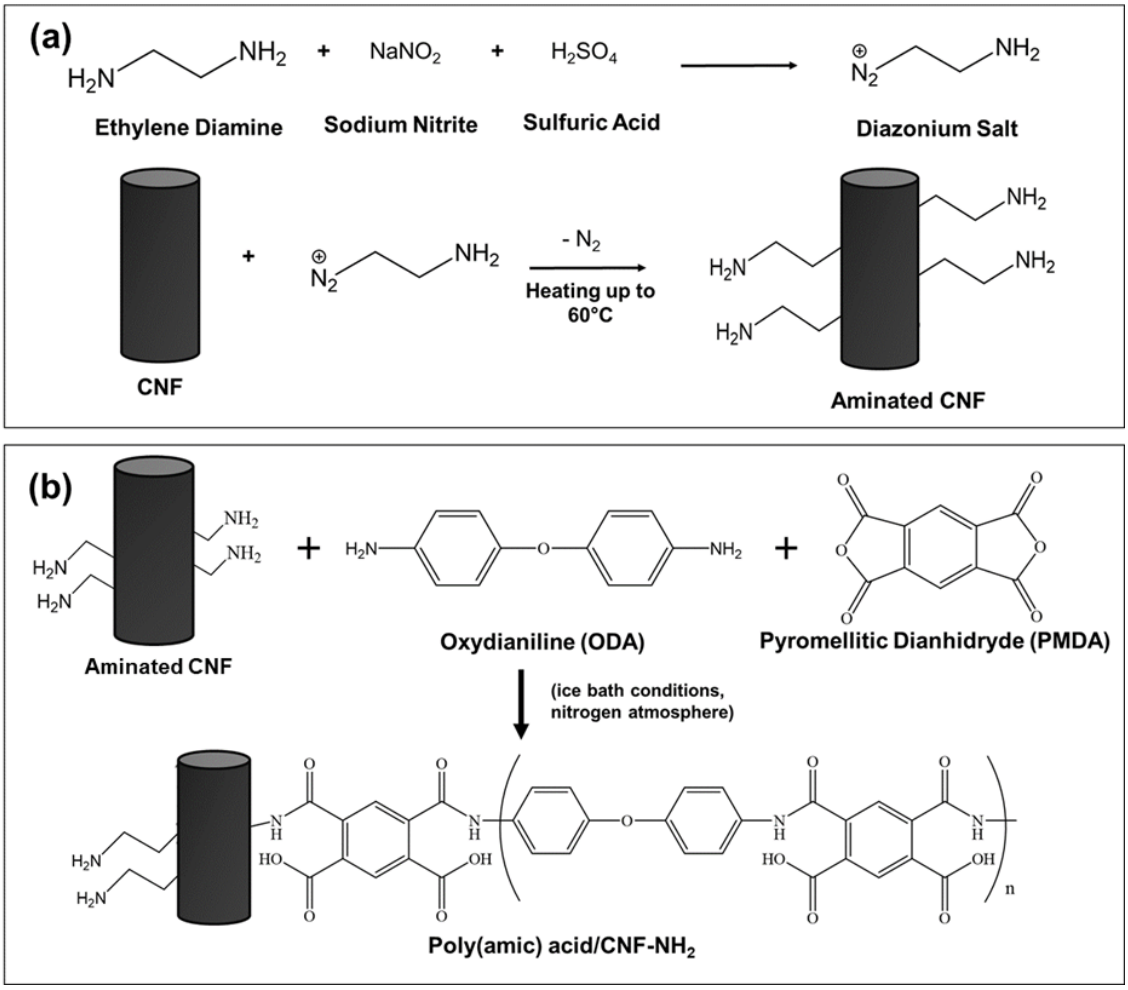

Figure 9. The Possible Reaction of (A) CNF Amination and (B) the Reaction of Aminated CNF, Oxydianiline (ODA), and Pyromellitic Dianhydride (PMDA) to Form Poly(Amic) Acid/CNF−NH_2

its original shape when the applied load is removed (Abdewi, 2017). The maximum load value linearly increases with increasing orderliness (how the composition of polymer matrices and filler is arranged orderly) (Amjadi and Fatemi, 2020), indicating that the higher the ultimate tensile strength, the better the material's ability to withstand a load. This property also might correlate with filler dispersion in polymer matrices when curing as a solid-phase composite. Compared with composites without fillers, the composites reinforced by CNF and aminated CNF fillers show a higher maximum load value than those without fillers. When the polymers used in the composites are ER and PI, this combination allows more oxygen-containing groups to bond between each polymer, resulting in better load values than the values in ER composites. In addition, the chemical bond between aminated CNF and polymer matrices gives the composite a better elongation ability. The N–H groups in aminated CNF connect through the covalent bond linking the CNF to C–O–C bonds in the PMDA, resulting in the imide bonds. Therefore, the ER/CNF−NH_2 has a lower maximum strain value than the ER-PI/CNF−NH_2, in which the PI combination with ER significantly enhances the maximum load by more than three times with different tensile displacement values.

Tensile displacement is defined as the strain deformation or elongation of a solid body due to applying a tensile force or stress. The increase in tensile strain indicates that the material is becoming more elastic. The decreasing value of the tensile strain suggests that the material is less flexible and will be fractured. As shown in Figure 8 (b and d), it is observable that even ER-PI composites have higher load values; they have lower displacement values than the displacement value in ER. However, their values are still significantly higher than those of ER composites with CNF and aminated CNF fillers, indicating that using fillers successfully reinforced the mechanical properties. Interestingly, the difference in displacement values between ER-PI composites with aminated and non-aminated filler is significantly higher than that of ER composites using similar fillers. The absence of the chemical bonds connecting the CNF

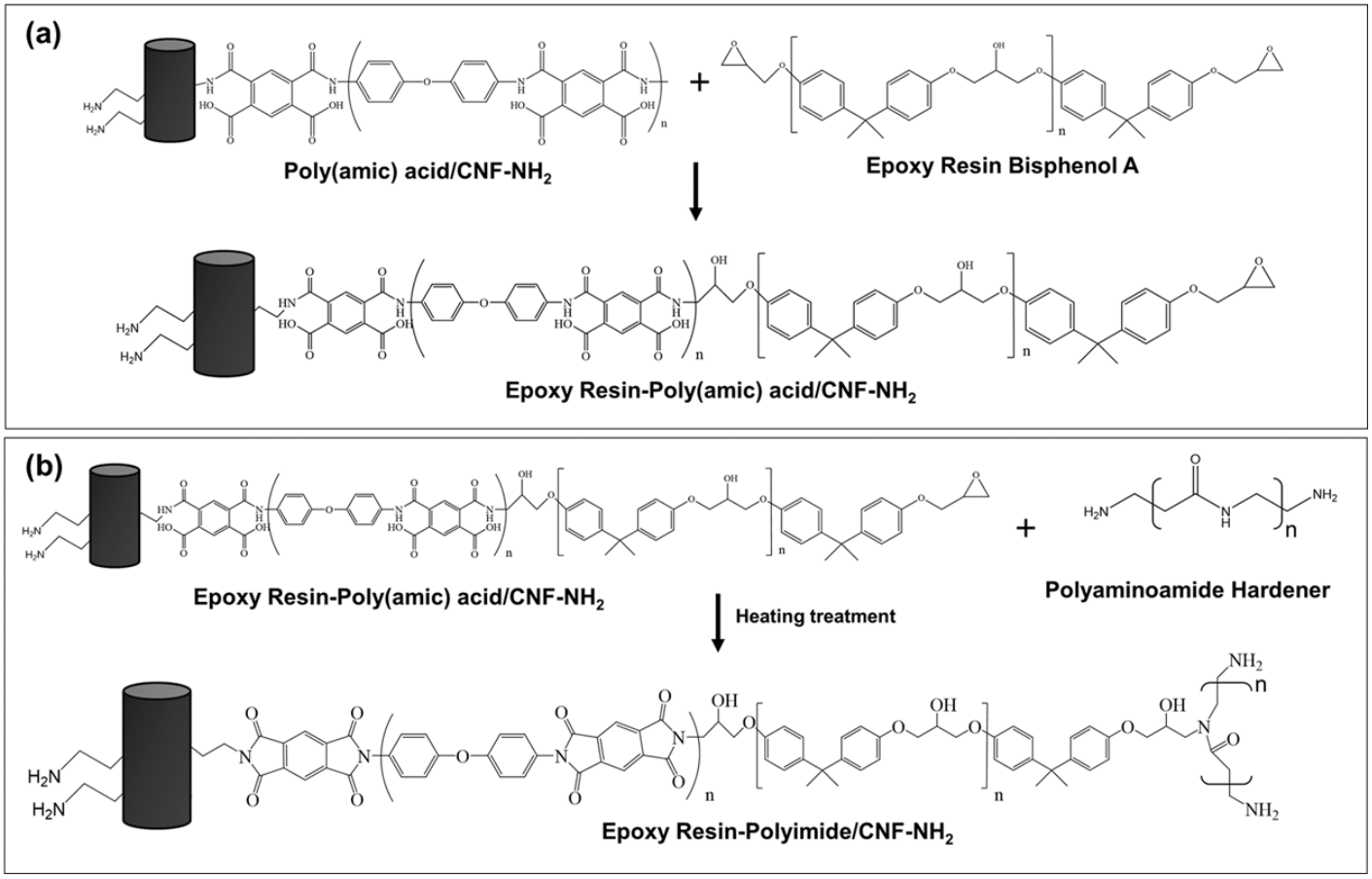

Figure 10. The Possible Reaction of (a) Poly(Amic)acid/Aminated CNF and Epoxy Resin, and (b) the Formation of Epoxy Resin-Polyimide/Aminated CNF Composites

fillers and polymer matrices made the composites unable to withstand the elongation. Therefore, ER-PI/CNF – NH_2 has the highest maximum displacement or strain among the composites with CNF fillers.

The possible reactions in all steps in preparing composites are shown in Figure 9 and Figure 10. Figure 9 (a) shows the preparation of aminated CNF through the reaction with ethylenediamine, sodium nitrite, and sulfuric acid, producing diazonium salt as the precursor of the amine group, which later attached to the CNF tube structure. The unstable diazonium salt tends to lose nitrogen (N_2 gas) and produce radical species that bond with reactive carbon in CNF, creating new covalent bonds containing amine groups (Yaghoubi and Ramazani, 2018). Figure 9 (b) shows the possible interaction between oxydianiline (ODA) and pyromellitic dianhydride (PMDA), resulting in the polyimide precursor (poly(amic) acid (PAA)) that will further bond the nucleophilic side of amine groups in CNF through epoxy groups in PMDA. PAA formation occurs through an exothermic polycondensation reaction in a dipolar solvent (dimethylacetamide). Figure 10 (a) shows the possible interaction of poly(amic) acid bonded to aminated CNF and bisphenol A (epoxy resin) through the bond created between the opened C–O–C epoxy group with N–H bond in poly(amic) acid. The epoxy ring opening possibly occurs via a reaction between it and secondary amine groups in the poly(amic) acid. The further possible interaction when the hardener is added is shown in Figure 10 (b), in which the end of C–O–C epoxy groups reacts with the N–H bond of polyaminoamide hardener. After heating treatment, the imidization occurs by closing the open ring in poly(amic acid), resulting in polyimide with bonds of –CO–N–CO– (Gaw et al., 1996). This process results in the extension of the polymer via homopolymerization of unreacted epoxide rings, creating the 3D epoxy network. The epoxy groups can also react with available free hydroxyl groups via crosslinking reactions (Gaw et al., 1996). Furthermore, during the curing process with the addition of polyaminoamide harderner, a 3D thermoset polymer further formed, resulting in multi-coordination sites between hydroxyl and amino groups (Dagdag et al., 2019).

4. CONCLUSIONS

CNF filler was successfully synthesized, purified, and modified with an amine group, possibly covalently attached to the carbon atoms. The SEM and TEM images show that the CNF resem-

bles bundle fibers that gathered overlapping with an average diameter of around 100-120 nm and become significantly narrower after purification. XRD data analysis shows that amine surface modification does not destroy the tube structure of CNF assigned by a similar diffraction profile as purified CNF. The FTIR analysis indicates the success of amine surface modification through covalent bonding of C–N (~1153 cm^{-1}), N–H (3737 cm^{-1}), primary amine N–H (1534 cm^{-1}) functional groups to C atoms in CNF structure. The dispersion test shows that modified CNF has better dispersion in water, strengthening the success of amination. The macroscopic images show that aminated filler makes a homogenous distribution in polymer matrices. The FTIR of composites shows the increasing intensity in the N–H, C=O amide, and C−H functional groups due to stronger covalent crosslinking bonds between polymers and aminated CNF filler. The TGA graph shows the most significant degradation in the termination of polyimide and epoxy resin. Adding aminated CNF filler increases the composites' hardness value and tensile values. The aminated CNF fillers in the composites create conductive pathways in epoxy resin-polyimide-insulated polymer matrices, increasing EMI absorption ability. The prepared composites in this study can be applied conclusively as electromagnetic shielding material.

5. ACKNOWLEDGMENT

We acknowledge financial support from Sebelas Maret University under research grant number 452/UN27.21/PN/2020 and number 260.UN27.22/HK.07.00/2021 by the Ministry of Research, Technology, and Higher Education of the Republic of Indonesia.

REFERENCES

Abbass, O. A., A. I. Salih, and O. M. A. Hurmuzy (2020). Study of the Mechanical and Physical Properties of Bio-Composite Material Based on Wheat Starch and Wheat Straw Fibers. *IOP Conference Series: Materials Science and Engineering*, **745**(1); 012075

Abdewi, E. F. (2017). Mechanical Properties of Reinforcing Steel Rods Produced by Zliten Steel Factory. In *Reference Module in Materials Science and Materials Engineering*. Elsevier

Ahmed, I., R. Jan, A. N. Khan, I. H. Gul, R. Khan, S. Javed, M. A. Akram, A. Shafqat, H. M. Cheema, and I. Ahmad (2020). Graphene-Ferrites Interaction for Enhanced EMI Shielding Effectiveness of Hybrid Polymer Composites. *Materials Research Express*, **7**(1); 016304

Amjadi, M. and A. Fatemi (2020). Tensile Behavior of High-Density Polyethylene Including the Effects of Processing Technique, Thickness, Temperature, and Strain Rate. *Polymers*, **12**(9); 1857

Bilisik, K., G. Erdogan, N. Karaduman, and E. Sapanci (2022). Developments of Multi-Nanostitched 3D Carbon/Epoxy Nanocomposites: Tensile/Shear and Interlaminar Properties. *Applied Composite Materials*, **29**(1); 3–26

Chen, D. S., C. H. Chen, W. T. Whang, and C. W. Su (2023). Interpenetration Networked Polyimide-Epoxy Copolymer Under Kinetic and Thermodynamic Control for Anticorrosion Coating. *Polymers (Basel)*, **15**(1); 243

Chen, Y., W. Wei, Y. Zhu, J. Luo, and X. Liu (2019). Non-covalent Functionalization of Carbon Nanotubes via Co-Deposition of Tannic Acid and Polyethyleneimine for Reinforcement and Conductivity Improvement in Epoxy Composite. *Composites Science and Technology*, **170**; 25–33

Dagdag, O., R. Hsissou, A. Berisha, H. Erramli, O. Hamed, S. Jodeh, and A. El Harfi (2019). Polymeric-Based Epoxy Cured with a Polyaminoamide as an Anticorrosive Coating for Aluminum 2024-T3 Surface: Experimental Studies Supported by Computational Modeling. *Journal of Bio- and Tribo-Corrosion*, **5**(3); 58

de Souza, G. and J. R. Tarpani (2021). Interleaving CFRP and GFRP with a Thermoplastic Ionomer: The Effect on Bending Properties. *Applied Composite Materials*, **28**(2); 559–572

Dhanasekar, S., T. J. Stella, A. Thenmozhi, N. D. Bharathi, K. Thiyagarajan, P. Singh, Y. S. Reddy, G. Srinivas, and M. Jayakumar (2022). Study of Polymer Matrix Composites for Electronics Applications. *Journal of Nanomaterials*, **2022**; 8605099

Duarah, R. and N. Karak (2015). A Starch Based Sustainable Tough Hyperbranched Epoxy Thermoset. *RSC Advances*, **5**(79); 64456–64465

Egbo, M. K. (2021). A Fundamental Review on Composite Materials and Some of Their Applications in Biomedical Engineering. *Journal of King Saud University - Engineering Sciences*, **33**(8); 557–568

Elsafi, M., N. Almousa, F. I. Almasoud, M. Almurayshid, A. R. Alyahyawi, and M. I. Sayyed (2022). A Novel Epoxy Resin-Based Composite with Zirconium and Boron Oxides: An Investigation of Photon Attenuation. *Crystals*, **12**(10); 1370

Eren, O., N. Ucar, A. Onen, N. Kizildag, and I. Karacan (2015). Synergistic Effect of Polyaniline, Nanosilver, and Carbon Nanotube Mixtures on the Structure and Properties of Polyacrylonitrile Composite Nanofiber. *Journal of Composite Materials*, **50**(15); 2073–2086

Gaw, K., M. Kikei, M.-A. Kakimoto, and Y. Imai (1996). Preparation of Polyimide-Epoxy Composites. *Reactive and Functional Polymers*, **30**(1); 85–91

Hashemi, S. A. and S. M. Mousavi (2016). Effect of Bubble Based Degradation on the Physical Properties of Single Wall Carbon Nanotube/Epoxy Resin Composite and New Approach in Bubbles Reduction. *Composites Part A: Applied Science and Manufacturing*, **90**; 457–469

Havigh, R. S. and H. M. Chenari (2023). Preparation and Characterization Study of γ-Fe_2O_3/Carbon Composite Nanofibers: Electrospinning of Composite Fibers Using PVP and Iron Nitrate as Precursors. *Physical Chemistry Chemical Physics*, **25**(12); 8684–8691

Hsissou, R., R. Seghiri, Z. Benzekri, M. Hilali, M. Rafik, and A. Elharfi (2021). Polymer Composite Materials: a Comprehensive Review. *Composite Structures*, **262**; 113640

Huang, L., X. Geng, H. Li, K. Jia, J. Liu, Z. Xue, A. Aydeng, W. Xi, and H. Liang (2023). Thermal Response of Carbon Fiber Reinforced Polyimide Composite Laminate Coated with Highly Oriented Graphite Film Under Heating on Single Side. *Applied Composite Materials*, **30**(3); 857–870

Iuvshin, A. M., S. D. Tretyakov, Y. S. Andreev, and I. N. Gibadullin (2020). Thermoplastic Polymer Composites Production by Automated Fiber Placement Method. *Key Engineering Materials*, **836**; 78–83

Jin, F.-L., X. Li, and S. Park (2015). Synthesis and Application of Epoxy Resins: A Review. *Journal of Industrial and Engineering Chemistry*, **29**; 1–11

Kanjana, N., W. Maiaugree, S. Tontapha, P. Laokul, A. Chingsungnoen, S. Pimanpang, I. Chaiya, S. Daengsakul, and V. Amornkitbamrung (2023). Effect of Carbonization Temperature on the Electrocatalytic Property and Efficiency of Dye-Sensitized Solar Cells Derived from Corncob and Sugarcane Leaf Agricultural Residues. *Biomass Conversion And Biorefinery*, **13**(9); 8361–8371

Kausar, A. (2020). Hybrid Polymeric Nanocomposites with EMI Shielding Applications. In K. Joseph, R. Wilson, and G. George, editors, *Materials for Potential EMI Shielding Applications*. Elsevier, pages 227–236

Khan, M., M. H. Younes, A. Zaib, U. Farooq, A. Khan, M. Zahid, and U. Hussan (2021). Investigation of Space Charge Behavior in Self-Healing Epoxy Resin Composites. *Journal Of Materials Science: Materials In Electronics*, **32**; 1–9

Khattak, M. J., A. Khattab, P. Zhang, H. R. Rizvi, and T. Pesacreta (2013). Microstructure and Fracture Morphology of Carbon Nano-Fiber Modified Asphalt and Hot Mix Asphalt Mixtures. *Materials And Structures*, **46**(12); 2045–2057

Kiran, M. D., H. K. Govindaraju, T. Jayaraju, and N. Kumar (2018). Review-Effect of Fillers on Mechanical Properties of Polymer Matrix Composites. *Materials Today: Proceedings*, **5**; 22421–22424

Kondawar, S. B. and P. R. Modak (2020). Chapter 2 - Theory of EMI Shielding. In K. Joseph, R. Wilson, and G. George, editors, *Materials for Potential EMI Shielding Applications*. Elsevier, pages 9–25

Kranauskaite, I., J. Macutkevic, A. Borisova, A. Martone, M. Zarrelli, A. Selskis, A. Aniskevich, and J. Banys (2018). Enhancing Electrical Conductivity of Multiwalled Carbon Nanotube/Epoxy Composites by Graphene Nanoplatelets. *Lithuanian Journal of Physics*, **57**(4); 232–242

Krauklis, A. E., C. W. Karl, A. I. Gagani, and J. K. Jørgensen (2021). Composite Material Recycling Technology—State-of-the-Art and Sustainable Development for the 2020s. *Journal of Composites Science*, **5**(1); 28

Lavagna, L., R. Nisticò, S. Musso, and M. Pavese (2021). Functionalization as a Way to Enhance Dispersion of Carbon Nanotubes in Matrices: A Review. *Materials Today Chemistry*, **20**; 100477

Li, Y., J. Li, W. Zhang, Q. Lin, L. Chen, Z. Weng, and Y. Xiao (2024). Rigid and Crosslinkable Polyimide Curing Epoxy Resin with Enhanced Comprehensive Performances. *Polymer*, **297**; 126836

Li, Y., G. Sun, Y. Zhou, G. Liu, J. Wang, and S. Han (2022). Progress in Low Dielectric Polyimide Film—A Review. *Progress in Organic Coatings*, **172**; 107103

Lim, J., S. Bee, L. T. Sin, C. T. Ratnam, and Z. A. A. Hamid (2021). A Review on the Synthesis, Properties, and Utilities of Functionalized Carbon Nanoparticles for Polymer Nanocomposites. *Polymers*, **13**(20); 3547

Lincon, M. I. and V. B. Chalivendra (2023). Dynamic Fracture Toughness and Damage Monitoring in Hybrid Composites. *Applied Composite Materials*, **30**(6); 1907–1928

Liu, Y., D. He, O. Dubrunfaut, A. Zhang, L. Pichon, and J. Bai (2021). In-Situ Growing Carbon Nanotubes on Nickel Modified Glass Fiber Reinforced Epoxy Composites for EMI Application. *Applied Composite Materials*, **28**(3); 777–790

Manikandan, M., R. Gunachandran, M. Vigneshwaran, S. Sudhakar, A. Srikanth, M. Venkateshkannan, M. Arivarasu, N. Arivazhagan, and D. N. Rajan (2017). Comparative Studies on Metallurgical and Mechanical Properties of Bimetallic Combination on Incoloy 800 and SS 316L Fabricated by Gas Metal and Shield Metal Arc Welding. *Transactions of the Indian Institute of Metals*, **70**(3); 749–757

Mieloszyk, M., K. Majewska, and W. Ostachowicz (2021). Application of Embedded Fibre Bragg Grating Sensors for Structural Health Monitoring of Complex Composite Structures for Marine Applications. *Marine Structures*, **76**; 102903

Moaseri, E., M. Karimi, M. Maghrebi, and M. Baniadam (2014). Two-Fold Enhancement in Tensile Strength of Carbon Nanotube–Carbon Fiber Hybrid Epoxy Composites Through Combination of Electrophoretic Deposition and Alternating Electric Field. *International Journal of Solids and Structures*, **51**(3); 774–785

Mohd Nurazzi, N., M. R. M. Asyraf, A. Khalina, N. Abdullah, F. A. Sabaruddin, S. H. Kamarudin, S. b. Ahmad, A. M. Mahat, C. L. Lee, H. A. Aisyah, M. N. Norrrahim, R. A. Ilyas, M. M. Harussani, M. R. Ishak, and S. M. Sapuan (2021). Fabrication, Functionalization, and Application of Carbon Nanotube-Reinforced Polymer Composite: An Overview. *Polymers*, **13**(7); 1047

Mokhtarifar, M., H. Arab, M. Maghrebi, and M. Baniadam (2017). Amine-Functionalization of Carbon Nanotubes Assisted by Electrochemical Generation of Chlorine. *Applied Physics A*, **124**(1); 21

Ogbonna, V. E., A. P. I. Popoola, O. M. Popoola, and S. O. Adeosun (2021). Recent Progress on Improving the Mechanical, Thermal and Electrical Conductivity Properties of Polyimide Matrix Composites from Nanofillers Perspective for Technological Applications. *Journal of Polymer Engineering*, **41**(9); 768–787

Ogbonna, V. E., A. P. I. Popoola, O. M. Popoola, and S. O. Adeosun (2023). A Review on Recent Advances on Improving Polyimide Matrix Nanocomposites for Mechanical, Thermal, and Tribological Applications: Challenges and Recommendations for Future Improvement. *Journal of Thermoplastic Composite Materials*, **36**(2); 836–865

Oladele, I. O., T. F. Omotosho, and A. A. Adediran (2020). Polymer-Based Composites: An Indispensable Material for Present and Future Applications. *International Journal of Polymer Science*, **2020**(1); 8834518

Pan, D., Q. Li, W. Zhang, J. Dong, F. Su, V. Murugadoss, Y. Liu, C. Liu, N. Naik, and Z. Guo (2021). Highly Thermal Conductive Epoxy Nanocomposites Filled with 3D BN/C Spatial Network Prepared by Salt Template Assisted Method. *Composites Part B: Engineering*, **209**; 108609

Potluri, R. and N. C. Krishna (2020). Potential and Applications of Green Composites in Industrial Space. *Materials Today: Proceedings*, **22**; 2041–2048

Qiao, Y., Q. Li, K. Yang, C. Bai, L. Zhang, Z. Yao, P. Wang, T. Zheng, X. Zhang, and X. Wang (2022). Improving Thermal Insulation Properties of Lightweight Epoxy Resin Matrix Composites with Millimeter-Sized Hollow Glass Microspheres/Epoxy Hollow Spheres. *Energy and Buildings*, **277**; 112546

Rajak, D. K., D. D. Pagar, R. Kumar, and C. I. Pruncu (2019). Recent Progress of Reinforcement Materials: A Comprehensive Overview of Composite Materials. *Journal of Materials Research and Technology*, **8**(6); 6354–6374

Ravishankar, B., S. K. Nayak, and M. A. Kader (2019). Hybrid Composites for Automotive Applications – A Review. *Journal of Reinforced Plastics and Composites*, **38**(18); 835–845

Ribeiro, H., M. C. Schnitzler, W. M. da Silva, and A. P. Santos (2021). Purification of Carbon Nanotubes Produced by the Electric Arc-Discharge Method. *Surfaces and Interfaces*, **26**; 101389

Setiawan, U. H., T. E. Saraswati, R. W. Lubis, and I. F. Nurcahyo (2023). Direct Growth of Long Magnetic Carbon Nanotubes on Incoloy Heating Elements and Its Hydrophilic Surface Modification by Atmospheric Pressure Plasma Jets. *Chemical Papers*, **77**; 5305–5316

Sezer Hicyilmaz, A. and A. C. Bedeloglu (2021). Applications of Polyimide Coatings: A Review. *SN Applied Sciences*, **3**(3); 363

Tarhini, A. and A. R. Tehrani-Bagha (2023). Advances in Preparation Methods and Conductivity Properties of Graphene-Based Polymer Composites. *Applied Composite Materials*, **30**(6); 1737–1762

Thangavel, P., S. Vignesh, R. Sureshkumar, A. Gowrishankar, and R. Girimurugan (2023). Study on Mechanical Properties of Polylactic Acid Matrix Added with Fly Ash and Tamarind Kernel Powder Micro Fillers. *NanoWorld Journal*, **9**(S1); S626–S630

Todor, M.-P., C. Bulei, and I. Kiss (2018). An Overview on Key Trends in Composite Materials Continuous Innovation and Improvements with Focus on Composites Based on Cellulose Fibers. *Acta Technica Corviniensis - Bulletin of Engineering*, **11**(4); 35–38

Tri-Dung, N. (2020). *Introduction to Composite Materials*, chapter 1. IntechOpen

Unnikrishnan, T. G. and P. Kavan (2022). A Review Study in Ultrasonic-Welding of Similar and Dissimilar Thermoplastic Polymers and Its Composites. *Materials Today: Proceedings*, **56**; 3294–3300

Wang, Z., S. Wu, J. Wang, A. Yu, and G. Wei (2019). Carbon Nanofiber-Based Functional Nanomaterials for Sensor Applications. *Nanomaterials*, **9**(7); 1045

Wu, N., Q. Hu, R. Wei, X. Mai, N. Naik, D. Pan, Z. Guo, and Z. Shi (2021). Review on the Electromagnetic Interference Shielding Properties of Carbon Based Materials and Their Novel Composites: Recent Progress, Challenges and Prospects. *Carbon*, **176**; 88–105

Xu, G., L. Tan, Y. Nie, X. Fang, and G. Chen (2023). Synthesis and Characterization of Epoxy Resin Composites Modified by Reactive Polyimide Containing Hydroxyl Groups. *High Performance Polymers*, **35**(9); 913–922

Yadav, D., F. Amini, and A. Ehrmann (2020). Recent Advances in Carbon Nanofibers and Their Applications – A Review. *European Polymer Journal*, **138**; 109963

Yaghoubi, A. and A. Ramazani (2018). Synthesis of Amino-Functionalized Carbon Nanotubes and Their Applications. *Current Organic Chemistry*, **22**(15); 1505–1522

Zhang, Y. and J. Gu (2022). A Perspective for Developing Polymer-Based Electromagnetic Interference Shielding Composites. *Nano-Micro Letters*, **14**(1); 89

Zhou, X., Y. Wang, C. Gong, B. Liu, and G. Wei (2020). Production, Structural Design, Functional Control, and Broad Applications of Carbon Nanofiber-Based Nanomaterials: A Comprehensive Review. *Chemical Engineering Journal*, **402**; 126189

Zhou, Z., N. Zhou, X. Jia, N. Liu, B. Shi, R. Jin, L. Qu, and B. Xu (2023). Research Progress of Filled-Type High-Thermal-Conductivity Flexible Polyimide Composites: A Review. *Journal of Materials Science*, **58**(41); 15973–16001

